ISSN (e): 2250 – 3005 || Volume, 14 || Issue, 3|| May. - June. – 2024 ||
International Journal of Computational Engineering Research (IJCER)

Comparison of2D and 3D models for numerical simulation of anchored secant pile wall for seismic Loading

Emuriat, J.E. (2024)
INES – Ruhengeri University of Applied Sciences
Faculty of Engineering and Technology
P.O.BOX 155Ruhengeri, Rwanda.

ABSTRACT:
Despite the efforts to invest heavily in infrastructure, the multi-storey buildings at the City Centers still lack adequate space for parking due to the associated high urbanization cost of land hence necessitating the need for deep excavation into the ground. The study provides a comparative analysis between 2D and 3D numerical modelling of anchored secant pile wallsunder dynamic loading conditions. The secant pile methodology comprised the formation of overlapping concrete piles. Plaxis 2D modelling in-plane strain is used in geometries that are more or less uniform cross-sections and corresponding stress states and loading schemes over a certain length perpendicular to the cross-section. Practically, this means that the 2D plane strain model considers one dimension to be relatively long. The 3D model alternative secant pile support system is not a plane strain condition because some 3D effects are not captured in a 2D plane strain model. Thus, the excavation geometry and loading conditions can only be fully modelled using 3D analysis. The loading condition was changed to be applied uniformly all around the perimeter of the excavation. This would simulate the construction condition and also act as the surcharge from the adjacent structures. The section forces obtained from the design of the excavation and those arising from the seismic action are compared for both 2D and 3D modelling. The dynamic analysis yields, the peak axial force of 4520 kN/m, which was 2.6% less than the design excavation force. The dynamic analysis yields a peak bending moment of 6860 kN/m, which was 1.6% higher than the design bending moment. The dynamic analysis yields a peak shear force of 2700 kN/m, which was 1.5% higher than the design shear force. The total displacement before the earthquake event for 2D and 3D are 0.94378E-3m and 0.1104E-3m respectively. The 3D yields 88.3% less than the 2D displacement under static load conditions. After the earthquake, the total displacement recorded for 2D and 3D are 38.05E-6m and 0.3375E-3m respectively. The 3D yields 88.7% more than 2D displacement under dynamic load conditions. The bigger difference could be due to the non-realistic modelling of the 2D.

Keywords – *FEM, Secant, Pile wall, Earthquake, Plaxis.*

Date of Submission: 13-05-2024 Date of acceptance: 25-05-2024

I. INTRODUCTION

The New headquarters building of the Commercial Bank of Ethiopia high-rise office tower complex consists of a 48-storey tower and a 5-level underground basement. The structure is like a cylinder with the exterior framework of steel structure and interior space filled with concrete, measuring 189.90m in height above the ground. The basement area is approximately 50500sq.m with 20m below the ground level. Providing space for parking, public amenities, etc. in multi-story buildings in urban settings has created the need for deep excavation into the ground to create additional floor space to meet the increasing space requirement. Structures near excavations, dense traffic scenarios, the presence of underground obstructions, and utilities have made excavations a formidable task to execute. Summarized information from case histories on ground settlements adjacent to excavations, the results indicated that settlements next to deep excavations are correlated to soil types [8]. Based on several case histories, the settlement profile is triangular for an extension in sandy soil or stiff clay [4]. The extensive empirical studies took 530 case histories of retaining wall and ground movement due to excavation in soft soil (C_u<75kPa). It was concluded that the ground conditions and excavation depth (H) are found to be the most influential parameters for deformation due to excavation [7]. Deep excavations are

supported by systems like conventional retaining walls, sheet pile walls, diaphragm walls, and secant pile walls. Secant piled walls are the preferred option near buildings,roads, and other sensitive structures. A secant pile wall is formed by the primary(female) and secondary(male) piles by drilling the piles to the specified diameter and required depth. The secondary pilesare positioned betweenthe primary piles and secant with the primary piles to form interlocking joints[6]. In the design and construction of circular secant pile walls in soft clay in Houston Texas, the finite element code Plaxis V8 was used in the study. The advanced hardening soil and Mohr coulomb model were used, and the reinforced concrete secant pile wall was modelled as a linear elastic plate element. The effective(drained) stiffness properties, modulus, and Poisson ratio, were used in the undrained and drained analysis. There was a reasonable agreement between the measured settlement of 6.0ft and the estimated end of primary settlement of 5.8ft [13]. Soft soils like normally consolidated clays, generally show a decreasing mean effective stress during undrained shearing, whereas the Mohr-Coulomb model would predict a constant effective stress during undrained in this case, which results in an over prediction of the shear strength [3]. The FEM predicts ground and support movements and the effects of excavation activities like dewatering, equipment surcharge, and stage construction on deformation and overall stability. Also, the discussion on the merits of numerical analysis in combination with Eurocode7 design approaches can be found in [2,10,11]. This study was a comparison between a 2D and 3D numerical analysis of a secant pile wall under dynamic loading conditions. A reference solution for a deep excavation problem utilizing the finite element method and an elastic-plastic constitutive model has been presented. The problem has been specified by the German Working Group 1.6 of the DGGT and has been used, in addition to the work presented here, as a benchmark problem [9]. Based on the reference solution a comprehensive study was performed to evaluate quantitatively the influence of various modelling assumptions on calculated displacements and bending moments. Some analysis assuming elastic – perfectly plastic material behavior confirmed the well-known fact that these very simple constitutive models are not well suited for predicting realistic deformations for this type of problem.The 2D plane strain, modelling assumes the out-of-plane geometry is large and or constrained and that the loading does not vary in the out-of-plane direction(Z), such that the Z-displacements are neglected, whereas 3D modelling takes width effect into account and provides insight into better modelling results than 2D finite element model. This study was focused on a comparison of 2D and 3D models for numerical simulation of anchored secant pile walls for seismic loading.

II. MATERIALS AND METHODS

This study involved a review of theories and important literature: the effect of deep excavation, the effect of supporting structures, secant pile walls, methods used in secant pile wall construction, case histories on secant pile walls, the design of composite materials and structures, potential geotechnical failures, constitutive models, response spectrum, seismic hazards in Ethiopia.

The effect of excavation geometry, such as excavation width, depth of the firm stratum, effect of wall stiffness, and the effect of wall embedment depth have been carried out by various researchers: Ng (1998) reported field measurements of a 10m excavation in over-consolidated stiff-fissured gault clay lion yard, Cambridge. Jen (1998) carried out numerical parametric studies to study the effects of excavation geometry, retaining system, and stress history of clay on ground deformations due to excavation.

Characterization of the soil to determine the input soil parameters used for modelling by applying the soil parameters and seismic parameters obtained from the geotechnical and seismic refraction report. Selection of an appropriate constitutive model and the input parameters. According to the constitutive model options available in Plaxis, the Hardening soil model with small strain stiffness (HS small) was used for dynamic analysis. However, the model does not include softening behavior under cyclic loading conditions and does not incorporate the liquefaction behavior under loading conditions [3]. A comparison of the modelling of 2D and 3D and important conclusions were drawn.

III. CONSTITUTIVE MODELS

Soil is a complicated material that behaves non-linearly and often shows anisotropic and time-dependent behavior when subjected to stresses. Generally, soil behaves differently in primary loading, unloading, and reloading. It exhibits non-linear behavior well below the failure condition with stress-dependent stiffness. Soil undergoes plastic deformation and is inconsistent in dilatancy and also experiences small strain stiffness at very low strains and upon stress reversal. In addition to soil behavior, its failure in a three-dimensional state of stress is extremely complicated. Numerous criteria have been derived to explain the condition for the failure of a material under such a loading state. Currently, various constitutive models for the soil have been developed and they cover a wider range of soil features, such as anisotropy, cyclic loading, creep, etc. The selection of a constitutive model for a geotechnical application depends on the mechanical properties of the soil and the stress changes that will occur in the future [14]. In the finite element analysis, reliable predictions can be achieved by using an appropriate constitutive model for a particular geotechnical problem. In

general, the criterion for the soil model evaluation should always be a balance between the requirements from the continuum mechanics aspect, the requirements of realistic presentation of soil behavior from the laboratory testing aspect, and simplicity in computational application.

IV. MODELLING

The detailed design for the lateral support and foundation was conducted by China State Engineering Corporation (CSEC), and included but was not limited to; soldier piles and shotcrete lagging techniques which retained the soil. The soldier piles were driven at intervals of 1800mm along the planned excavation perimeter (Figure 24). The lagging consisted of steel mesh inserted behind the front pile flanges as the excavation proceeded and concrete of grade C-20 was sprayed to the lagging. The wall was designed to receive additional support from the anchors of different free and bonded lengths placed in layers. This study is focused on investigating the shoring system of the Commercial Bank of Ethiopia using the secant pile wall as an alternative scheme.

4.1 Secant Pile Model

The alternative model shown in Figure 3 presents the layout of the secant piles as per the site drawing used for the construction (Figure 24).The secant pile wall consists of reinforced secondary (male) and unreinforced primary (female) as shown in Figure 1.

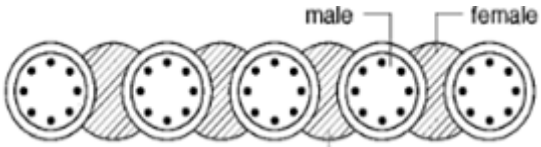

Figure 1: Typical secant pile wall arrangement with female(primary) and male(secondary) piles forming hard/soft wall after Suckling et al. (2005).

The components of the secant pile retaining wall are illustrated in Figure 2. The structure consists of wall-facing, anchors, tendons, and anchor heads that provide the connection of the tendon to the wall-facing. The anchor transmits a tensile force from the main structure through the anchor tendons to the surrounding ground. The shear strength of the ground is used to resist the tensile force. The anchors are composed of a fixed length that is bonded to the grout and an unbounded free length that transfers the lateral earth force from the wall to the anchorage. The anchor tendons were constructed of prestressed steel in the form of threaded bars.

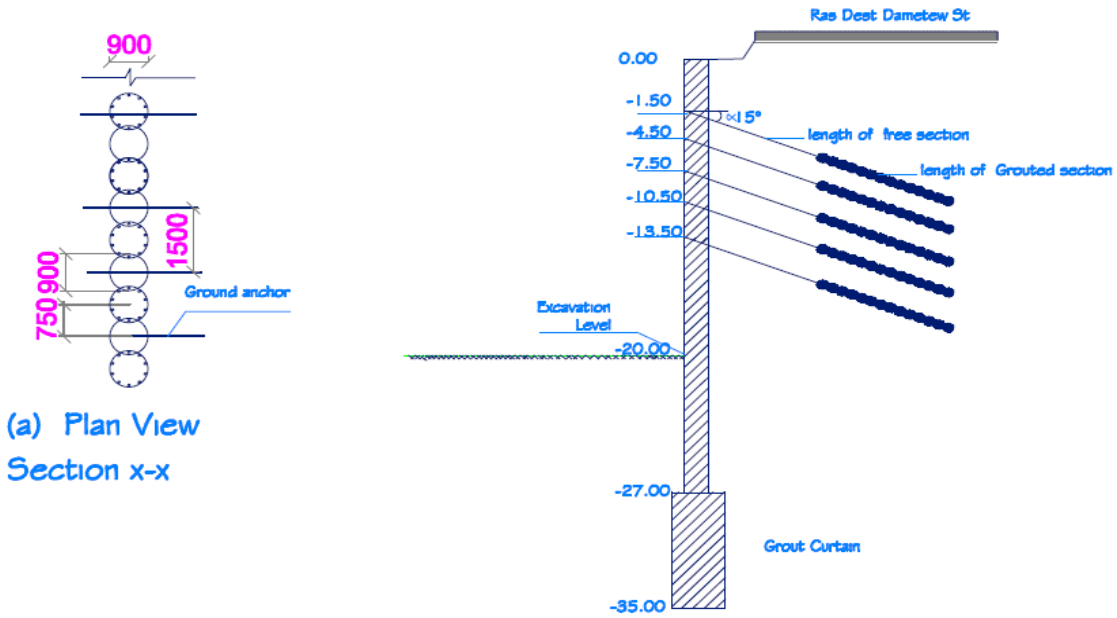

Figure 2: Cross section of the secant pile wall as the alternative scheme [5]

4.2 Secant Pile Merits

The main advantages of secant pile walls are: toincrease construction alignment flexibility, increase wall stiffness compared with sheet piles, can be installed in difficult ground (cobbles/ boulders), they are primarily used in unsuitable ground conditions or where there a high-water table condition without excessive dewatering.

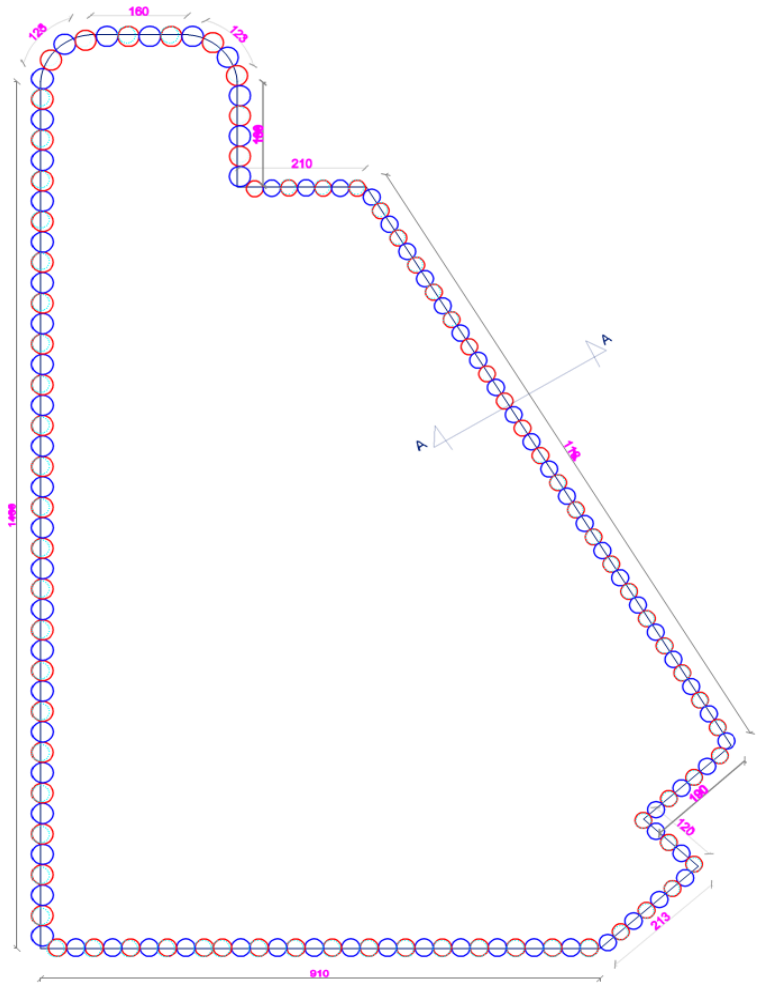

Figure 3: Site layout for the alternative wall scheme for using secant pile wall (All dimensions in cm) [5]

4.3 Selection of an appropriate constitutive model and input parameters

Based on the data collected for the Commercial Bank of Ethiopia, the site parameters are not elastic in behavior. Their inelastic behavior under cyclic loading can be described by elastic–plastic constitutive models. According to the constitutive model options available in Plaxis, the Hardening soil model with small strain stiffness (HS small) was used for dynamic analysis. However, the model does not include softening behavior under cyclic loading conditions and does not incorporate the liquefaction behavior under loading conditions [3].

4.4 Soil and material parameters

The original site information was obtained from the geotechnical report for the Commercial Bank and the P-wave refraction result along the weak profile was obtained from the seismic refraction report furnished by the seismology department at Arat Kilo – Addis Ababa University, Ethiopia. The analysis of geotechnical earthquake engineering requires the characterization of the dynamic soil properties using geophysical method. Figure 4and Figure 5 show P-wave refraction results along profiles 1 and 2. The coordinates of the two geophysical survey profiles are 473005E/996598N – 472997E/996723N (Profile - 1) and 473000E/996724N – 473048E/996646 (Profile -2). The ground surface was well leveled and the altitude is about 2332m above mean sea level. Before the excavation commencement of the geophysical surveys, the construction site was excavated to a depth of 20.0m

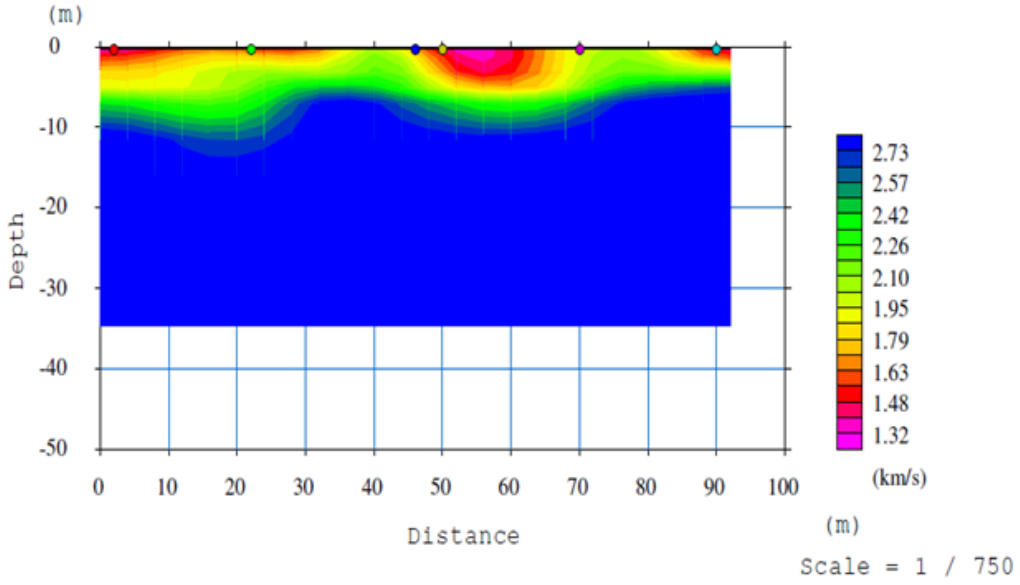

Figure 4: P-wave refraction results along profile 1, which clearly shows indentation with relatively low velocity in the middle for the CBE New building site [1].

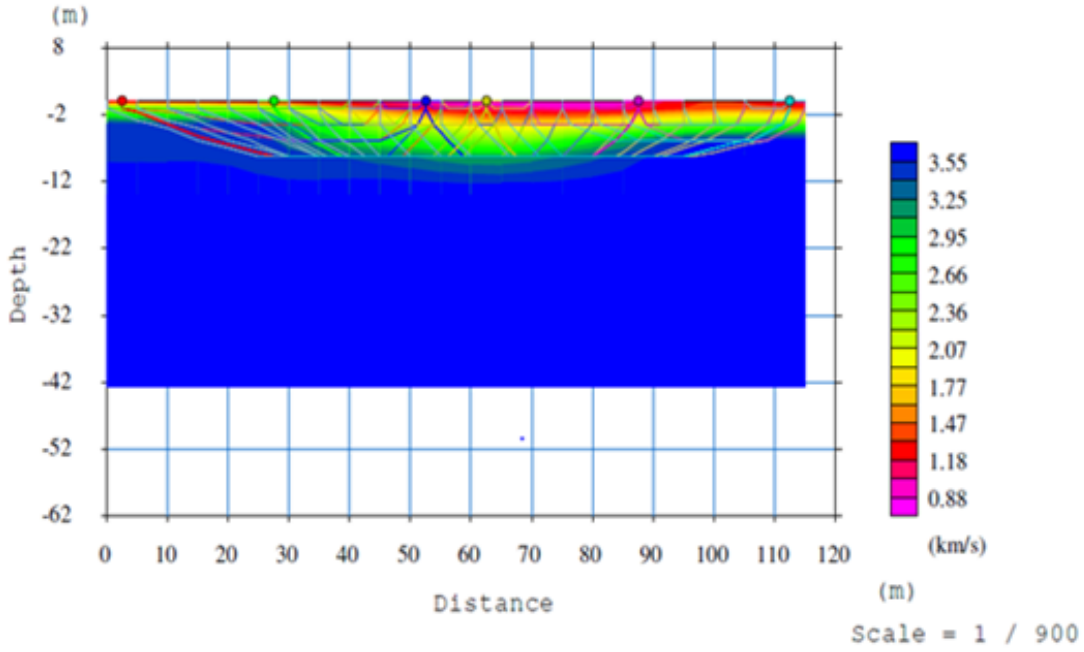

Figure 5: P-wave refraction results along profile 2. The P-wave velocity values are shown by the color-coded legend and the lines are the seismic ray paths the traversed or scanned medium for the CBE New building site [1].

Characterization of the soil to determine the input soil parameters used for the modelling by applying the soil parameters and seismic parameters obtained from the geotechnical investigation report and the seismic refraction test conducted by the Design and Share Company Limited and Seismology Department of Addis Ababa University respectively. Table 1 and Table 2. Furthermore, the engineering properties of the composite secant pile wall were obtained from the material properties from the catalog of the manufacturer and to determine the composite properties of the material by combining Young's modulus, shear modulus, and Poisson's ratio using Halpin – Tsai Equation.

Table 1: Summary of ground conditions encountered in boreholes [5]

STRATA DESCRIPTION	Elv	E_{50}	E_{Oed}	E_{ur}	γ_{uns}	γ_{sat}	c^{ref}	φ	m	R_{int}
	m	MPa			kN/m^3		MPa	deg	–	
Soft, organic silty CLAY	4.00	4.00	4.00	12.00	12.4	14.7	0.015	13	1.00	1.00
Silty CLAY	6.60	4.00	4.00	12.00	13.8	15.3	0.02	17	0.90	0.95
Highly weathered BASALT	8.80	2770	2770	8310	22.6	32.7	7.8	33	0.90	0.95
Medium strong, intensively fract to fragmented slightly to moderately weather BASALT	15.00	20630	20630	61890	24	35	18	34	0.70	0.80
Silty CLAY	18.20	4.00	4.00	12.00	12.4	14.2	0.02	17	0.90	0.95
Stiff, sandy clayey SILT	21.00	4.00	4.00	12.00	14.2	16.7	0	28	0.85	0.90
Highly weathered scoriaceous BASALT, decomp to silty CLAY	25.50	630	630	1890	22.4	32.9	13.6	32	0.90	0.95
Moderately weathered BASALT	39.00	20630	20630	61890	23.9	34.5	26	36	0.70	0.80
Stiff, swelling clayey SILT	45.00	4.00	4.00	12.00	15.3	17.4	0.015	22	0.90	0.95
Moderately weathered BASALT	52.00	2063	2063	6189	24	35	26	35	0.70	0.80
Strong, slightly fractured, fresh to faintly weathered BASALT	61.00	46510	46510	139530	25.7	36.8	29	38	0.50	0.60
Moderately weathered Basalt	75.00	20630	20630	61890	24	35	25	34	0.70	0.80
Strong, slightly fractured, fresh to faintly weathered BASALT	83.00	46510	46510	139530	26	37	29	38	0.50	0.60

Table 2: Summary of seismic properties encountered in boreholes [5]

STRATA DESCRIPTION	Elv	V_p	V_s	E_{ur}	G_{ur}	G_0	E_0	γ_{sat}	μ	G_0/G_{ur}
	m	m/s			GPa			kN/m^3	–	–
Soft, organic silty CLAY	4.00	1790	731	0.012	0.005	8E-04	0.002	14.7	0.30	0.1735
Silty CLAY	6.60	1950	796	0.012	0.005	1E-03	0.003	15.3	0.30	0.2141
Highly weathered BASALT occassionally, fresh rock present	8.80	2100	1277	8.31	3.272	0.005	0.014	32.7	0.27	0.0017
Moderately weathered BASALT	15.00	2730	1555	61.89	24.56	0.009	0.022	35	0.26	0.0004
Silty CLAY	18.20	2730	1115	0.012	0.005	0.002	0.005	14.2	0.30	0.3896
Stiff, sandy clayey SILT	21.00	2730	1672	0.012	0.005	0.005	0.011	16.7	0.20	0.9518
Highly weathered scoriaceous Basalt, decomp to silty CLAY	25.50	2730	1719	1.89	0.744	0.01	0.025	32.9	0.27	0.0133
Moderately weathered BASALT	39.00	2730	1719	61.89	24.37	0.01	0.026	34.5	0.27	0.0004
Stiff, swelling clayey SILT	45.00	2730	1672	0.012	0.005	0.005	0.012	17.4	0.20	0.9917
Moderately weathered Basalt	52.00	2730	1719	61.89	24.37	0.011	0.027	35	0.27	0.0004
Strong, slightly fractured, fresh to faintly weathered BASALT	61.00	2730	1689	139.5	58.61	0.011	0.025	36.8	0.19	0.0002
Silty CLAY	62.00	2730	1115	0.012	0.005	0.002	0.005	15	0.30	0.4115
Moderately weathered BASALT	75.00	2730	1555	61.89	24.56	0.009	0.022	35	0.26	0.0004
Strong, slightly fractured, fresh to faintly weathered BASALT	83.00	2730	2730	139.5	58.61	0.028	0.067	37	0.19	0.0005

4.5 Model geometry

The soil stratum consists of various layers of soil and decomposed basalt with 83.0m depth as determined from the SPT result. The soil stratigraphy, the general water level, and the initial conditions of the soil layers were considered in the modelling. A finite element numerical analysis using non-linear time history dynamic analysis was performed by using Plaxis 2D & 3D software. Figure 6shows the finite element model of the spoil strata. In the study, the soil strata were subjected to real earthquake waves (upland earthquake) which occurred in 1989. Figure 7shows the acceleration time history for the Loma Prieta earthquake. In a 2D model,

plane strain elements with 15 nodes and Hardening soil mode were used to model the soil. Tension cut-off was used to prevent the tensile stress which is not allowed in the soil element during the analysis.

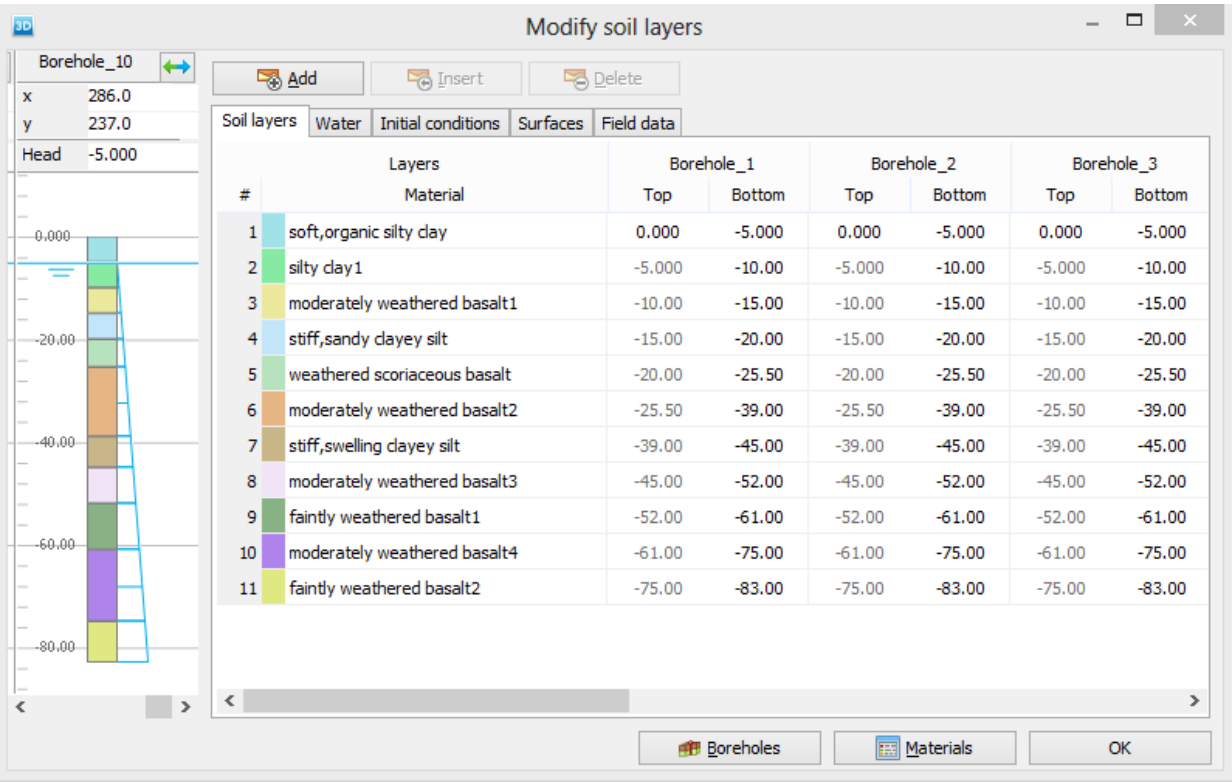

#	Material	Borehole_1 Top	Borehole_1 Bottom	Borehole_2 Top	Borehole_2 Bottom	Borehole_3 Top	Borehole_3 Bottom
1	soft,organic silty clay	0.000	-5.000	0.000	-5.000	0.000	-5.000
2	silty clay1	-5.000	-10.00	-5.000	-10.00	-5.000	-10.00
3	moderately weathered basalt1	-10.00	-15.00	-10.00	-15.00	-10.00	-15.00
4	stiff,sandy clayey silt	-15.00	-20.00	-15.00	-20.00	-15.00	-20.00
5	weathered scoriaceous basalt	-20.00	-25.50	-20.00	-25.50	-20.00	-25.50
6	moderately weathered basalt2	-25.50	-39.00	-25.50	-39.00	-25.50	-39.00
7	stiff,swelling clayey silt	-39.00	-45.00	-39.00	-45.00	-39.00	-45.00
8	moderately weathered basalt3	-45.00	-52.00	-45.00	-52.00	-45.00	-52.00
9	faintly weathered basalt1	-52.00	-61.00	-52.00	-61.00	-52.00	-61.00
10	moderately weathered basalt4	-61.00	-75.00	-61.00	-75.00	-61.00	-75.00
11	faintly weathered basalt2	-75.00	-83.00	-75.00	-83.00	-75.00	-83.00

Figure 6: Soil profile in plaxis3D Model

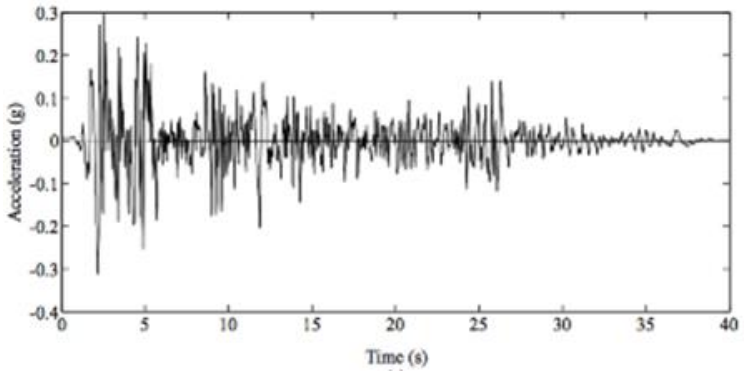

Figure 7: Real-time accelerogram of Del Valle Dam – Loma Prieta Earthquake

4.6 Base case model and mesh setup

The project data from the project drawings were initially used to develop a 3D geometric model to represent the construction process by reconciling field reports and simulating the actual construction process of the project. The refinement of the mesh affects the calculation results in the FE Analysis. The refinement of the mesh is also related to the calculation time. The large mesh elements generated require a large calculation time due to the stiffness matrices. The balance between accuracy and efficiency is key to the mesh setup. In Plaxis 3D, the mesh is generated automatically with the global refinement as set in Figure 8. The model is based on the site dimensions and the actual conditions. The resulting finite element model presents a close approximation to the original geometric model with Plaxis 3D.

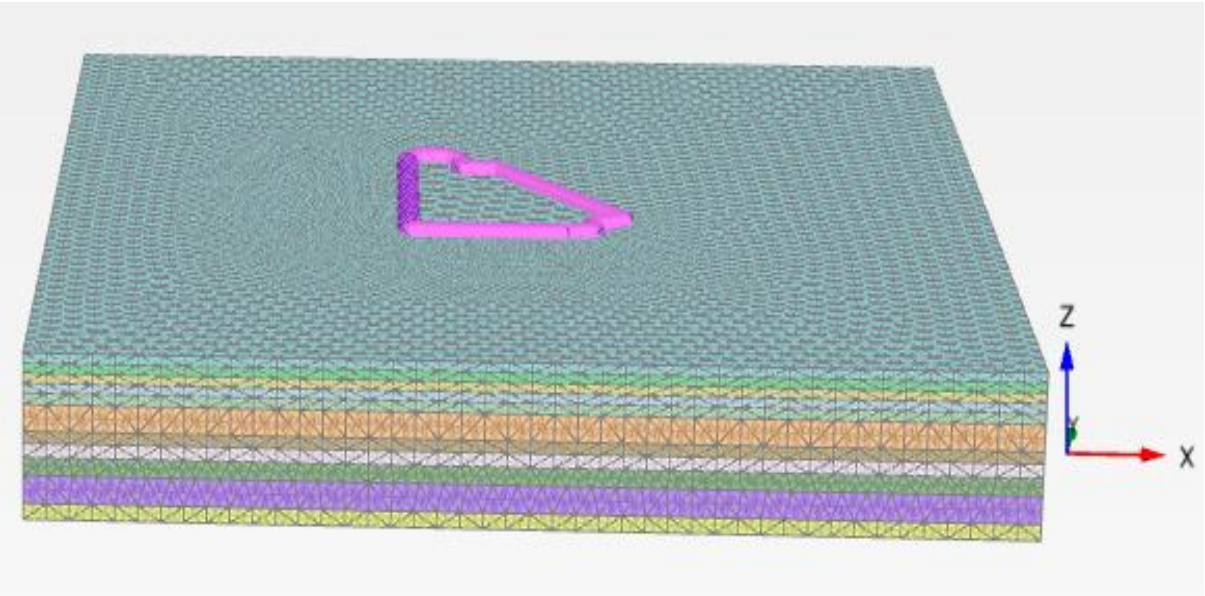

Figure 8: 3D Finite element mesh

4.7 Static loading

Due to the existence of several buildings around the excavation and the associated traffic, a large surcharge load is expected to take care of the adjoining structures and the traffic loading. Since the existing site surcharge could not be estimated accurately, the applied overload of 150 kPa was used for modelling. This load was also used in 3D finite element analysis of a deep excavation for the Odeon project in Monaco [12].

4.8 Dynamic loading

To simulate the actual condition, the dynamic load considered in this study was the upland earthquake of 18 October 1989 of real accelerogram which occurred at the Del Valle Dam Station. The finite element analysis with Plaxis 3D software was applied. The real accelerogram of strong motion was assigned as the dynamic multiplier and the generated spectrum was adjusted to the ground acceleration of 0.12g for the case of the Addis Ababa area.

4.9 Seismic hazard and response spectrum for Addis Ababa

The probabilistic Seismic Hazard Assessment (PSHA) combines seismic source zoning, earthquake recurrence, and ground motion attenuation to produce hazard curves in terms of level ground motion and associated annual frequency of exceedance. The results are expressed in terms of Uniform Hazard Response Spectra (UHRS) which are represented for a fixed probability of exceedance (return period), the value of the ground motion parameters versus the structural period with 5% damped UHRS on the rock are computed from a return period of 475 years.Figure 9shows the UHRS spectra for the 475-year return period in Addis Ababa City. Response spectrum can be interpreted as the locus of maximum response of a Single Degree of Freedom (SDOF) system for a given damping ratio. Response spectra thus help in obtaining the peak structural response under linear range, which can be used for obtaining lateral forces developed in structure due to earthquakes thus, facilitatingthe earthquake-resistant design of structure. Usually, the response of an SDOF system is determined by the time domain of frequency domain analysis, and for a given period of the system, the maximum response is picked.Figure 10shows response spectra with damping ratios.

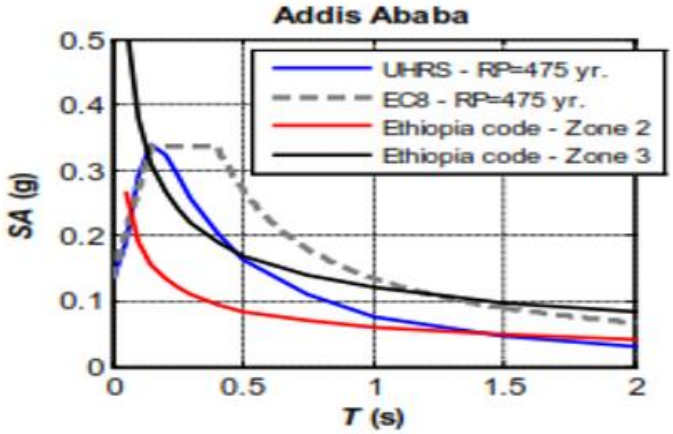

Figure 9: Uniform Hazard Spectra at Addis Ababa (blue curves) compared with elastic acceleration spectra from EN 1998 based on the PGA from RP = 475yr.and country seismic code criteria.
Source: 2nd European Conference on Earthquake Engineering and Seismology, Istanbul Aug.25-29, 201

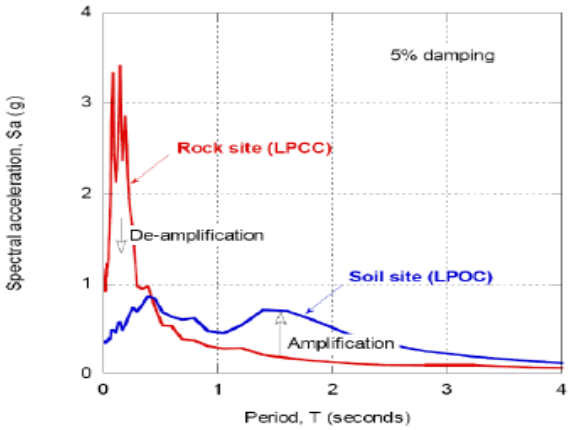

Figure 10: Acceleration response spectra during the 22 February 2011 Christchurch earthquake (Cubrinovski and McMahon 2011).

4.10 Comparison of the Results from a 2D and a 3D Model

The dynamic analysis of the NewCommercial Bank of Ethiopia building was performed using the 2D and 3D Plaxis Finite Element Analysis software. The Plaxis 2D is used to carry out analysis of deformations and stability problems for different geotechnical situations in two dimensions. However, when the 3D problem to be investigated is simplified into 2D, there is the possibility of obtaining matching results.

The total displacement before the earthquake event for the 2D and 3D are 0.94378E-3m and 0.1104E-3m respectively. The 3D yields 88.3% less than the 2D displacement under static load conditions. After the earthquake, the total displacement recorded for the 2D and 3D are 38.05E-6m and 0.3375E-3m respectively. The 3D yields 88.7% more than the 2D displacement under dynamic load conditions. The bigger difference could be due to the non-realistic modelling of the 2D. Furthermore, 2D plane strain modelling assumes the out-of-plane geometry is large or constrained and that the loading does not vary in the out-of-plane direction(z), such that the Z-displacements are neglected, whereas 3D modelling takes width effect into account and therefore provides insight into better modelling results than 2D finite element model.

The 2D modelling in-plane strain is used in geometries that are more or less uniform cross sections and corresponding stress states and loading schemes over a certain length perpendicular to the cross-section (Z-direction). Practically, this means that the 2D plane strain model considers one dimension to be relatively long.

The 3D model alternative secant pile support systems clearly not a plane strain situation because some 3D effects are not captured in the 2D plane strain model. Thus, the excavation geometry and loading conditions can only be fully modelled using Plaxis 3D analysis.

The analysis for stage excavation indicated that the maximum displacement (U_z) for 20m and 5m excavation depth was 0.1104E-3m and 0.02785E-3m respectively for static load condition in 2D.

The dynamic analysis also resulted to displacement (U_z) for 20m and 5m excavation depths as respectively 0.1104E-3m and 0.04542E-3m. This analysis revealed that the deeper the foundation excavation was, the larger the deformation. Since the excavation width is very wide, it also follows that the wider the

excavation, the larger the deformation.Also, the dynamic analysis for stage excavation indicated that for the same material property the deformation increases with increase in excavation depth in the Z-direction. The displacement at 5m and 10m stage excavation was respectively 0.04542E-3m and 0.03969E-3m. This further revealed that soft soil material is displaced more than the firm material during the earthquake event.

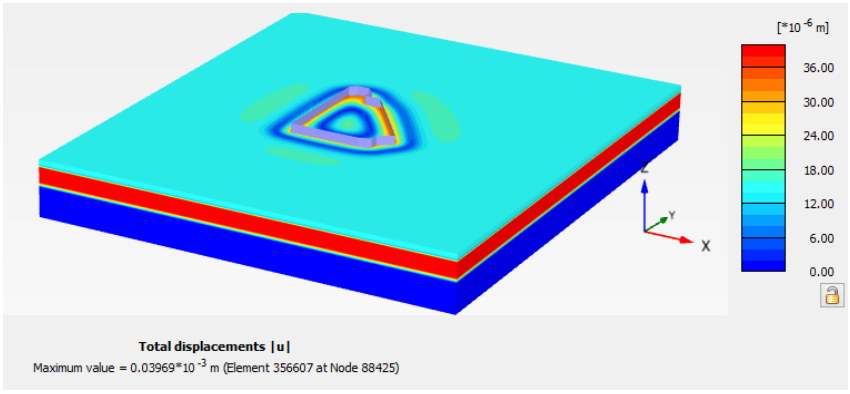

Figure 11: 3D Stage excavation 10m (Total displacement)

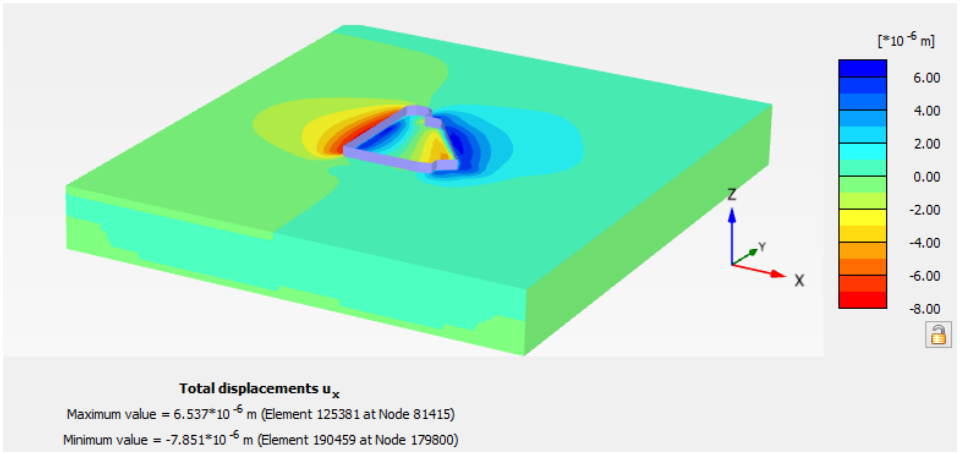

Figure 12: 3D Stage excavation 10m (Horizontal displacement)

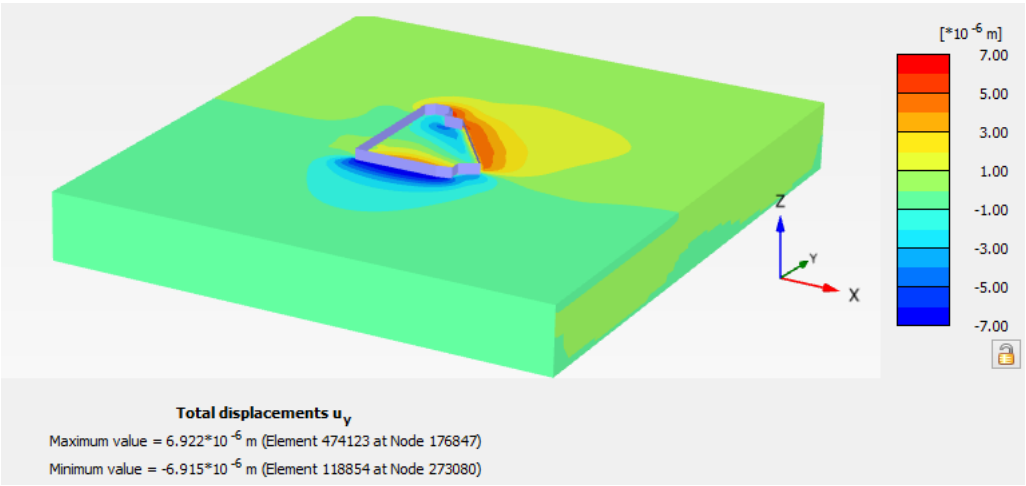

Figure 13: 3D Stage excavation 10m (Vertical displacement)

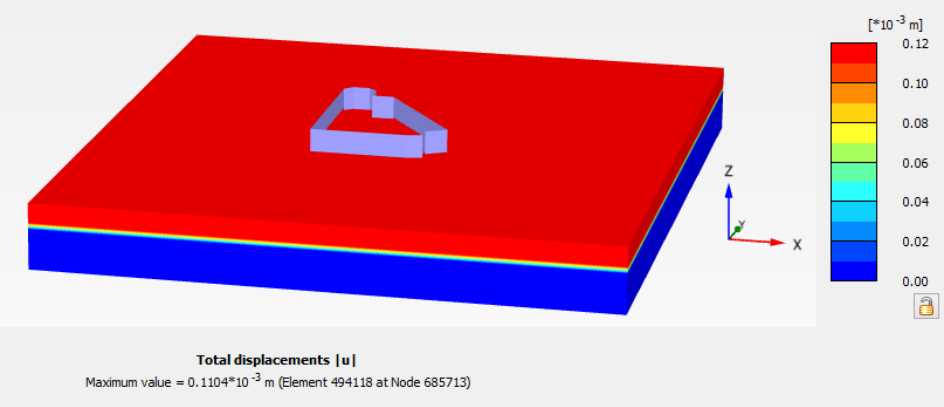

Figure 14: 3D Total displacement under static load condition

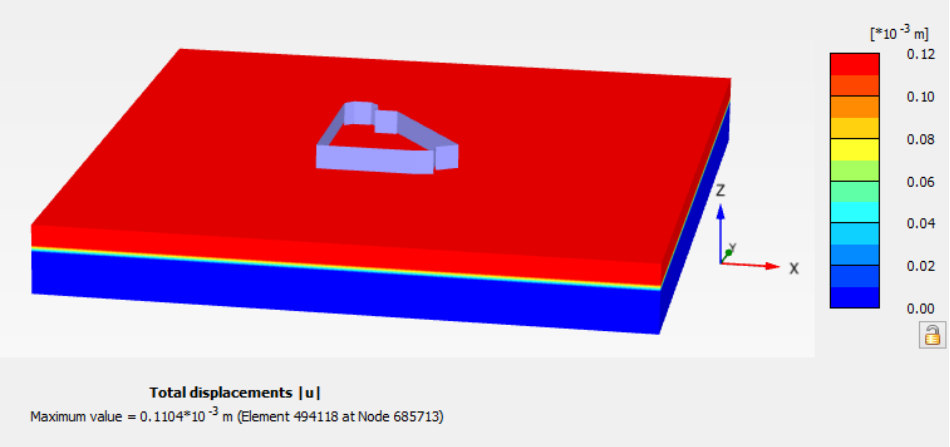

Figure 15: 3D Total displacement under dynamic load condition

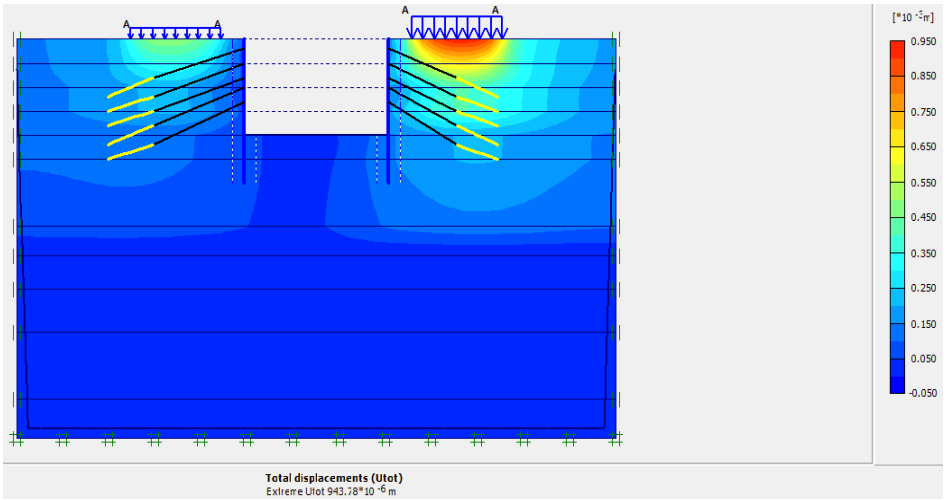

Figure 16: 2D Total displacement under static load condition

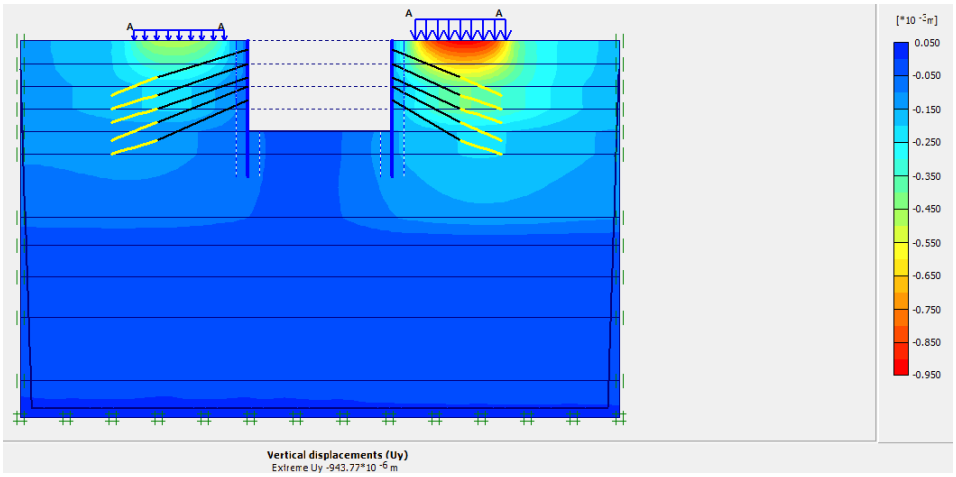

Figure 17: 2D Vertical displacement under static load condition

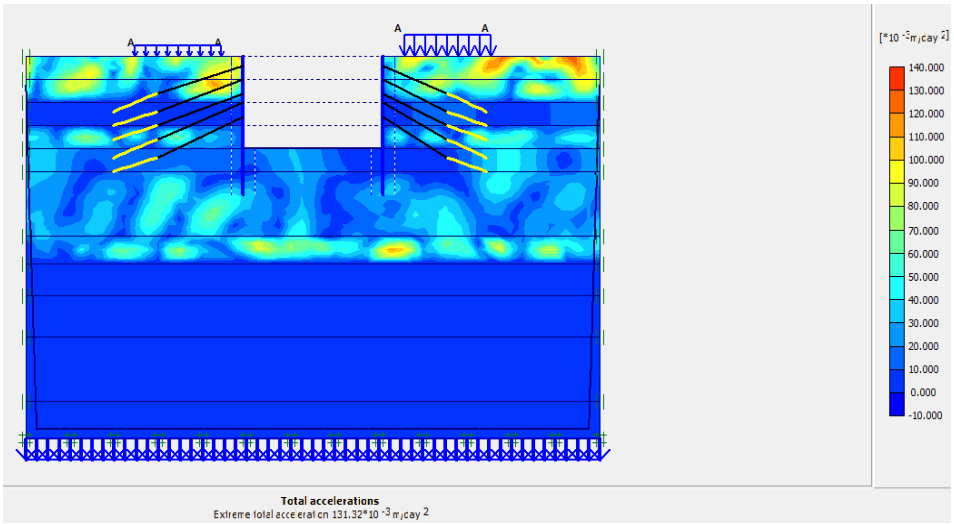

Figure 18: 2D Total acceleration under dynamic load condition

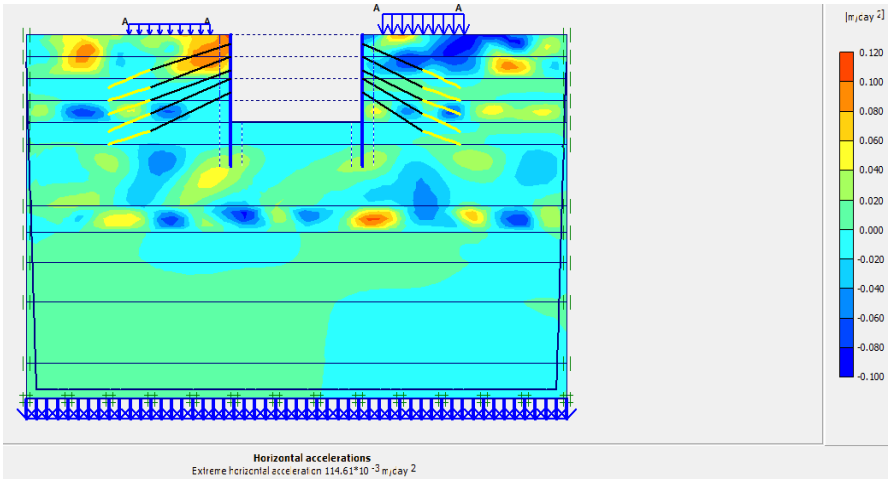

Figure 19: 2D Horizontal acceleration under dynamic load condition

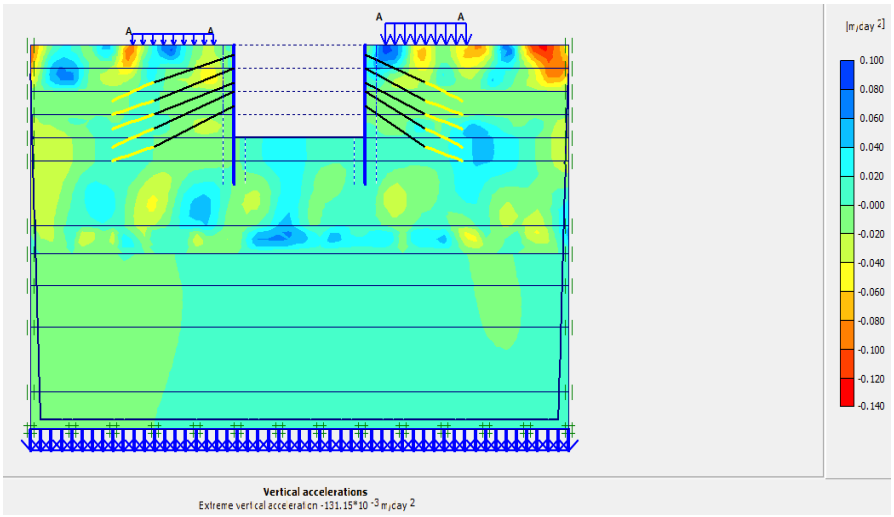

Figure 20: 2D Vertical acceleration underdynamic load condition

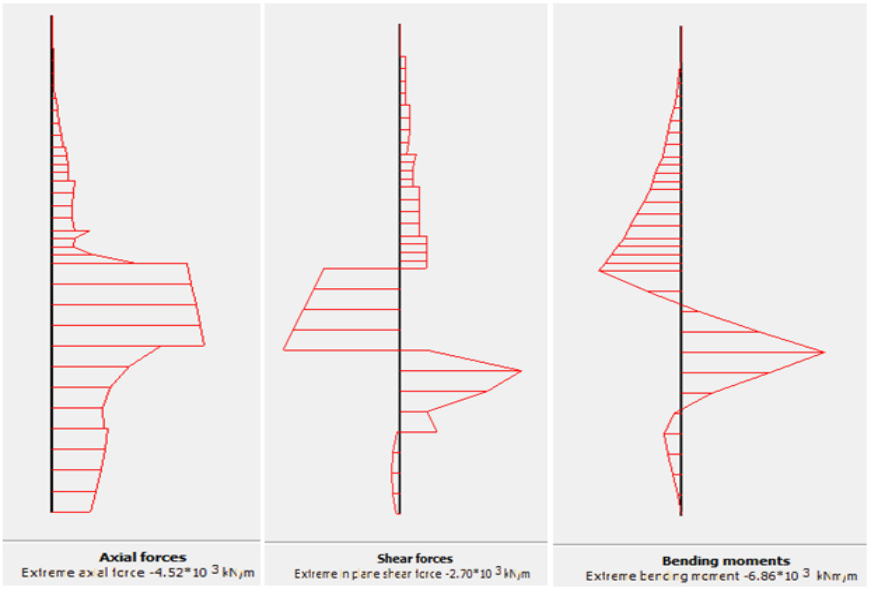

Figure 21: 2D Peak axial, bending and shear forces under dynamic load condition

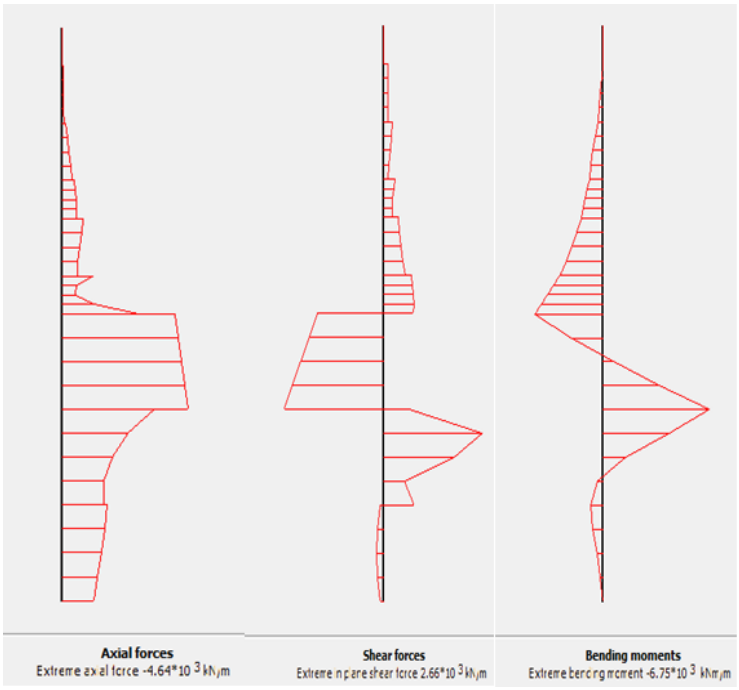

Figure 22: 2D Peak axial, bending and shear forces under static load condition

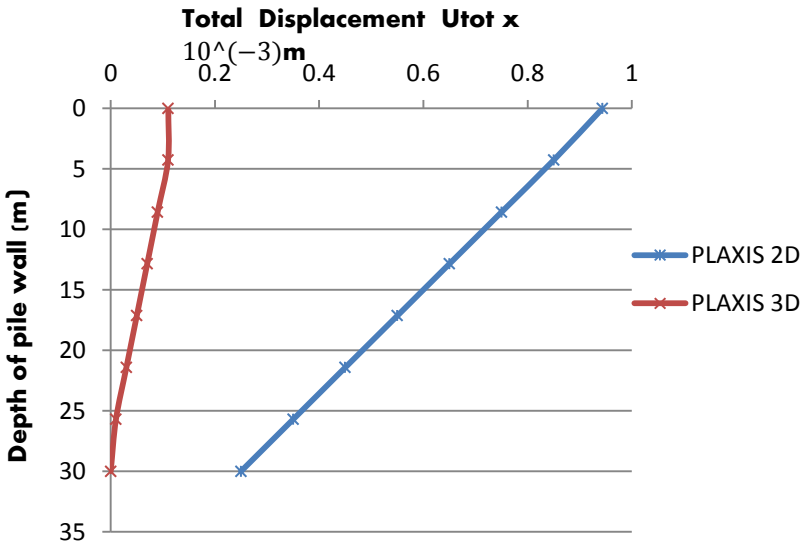

Figure 23: Static load condition

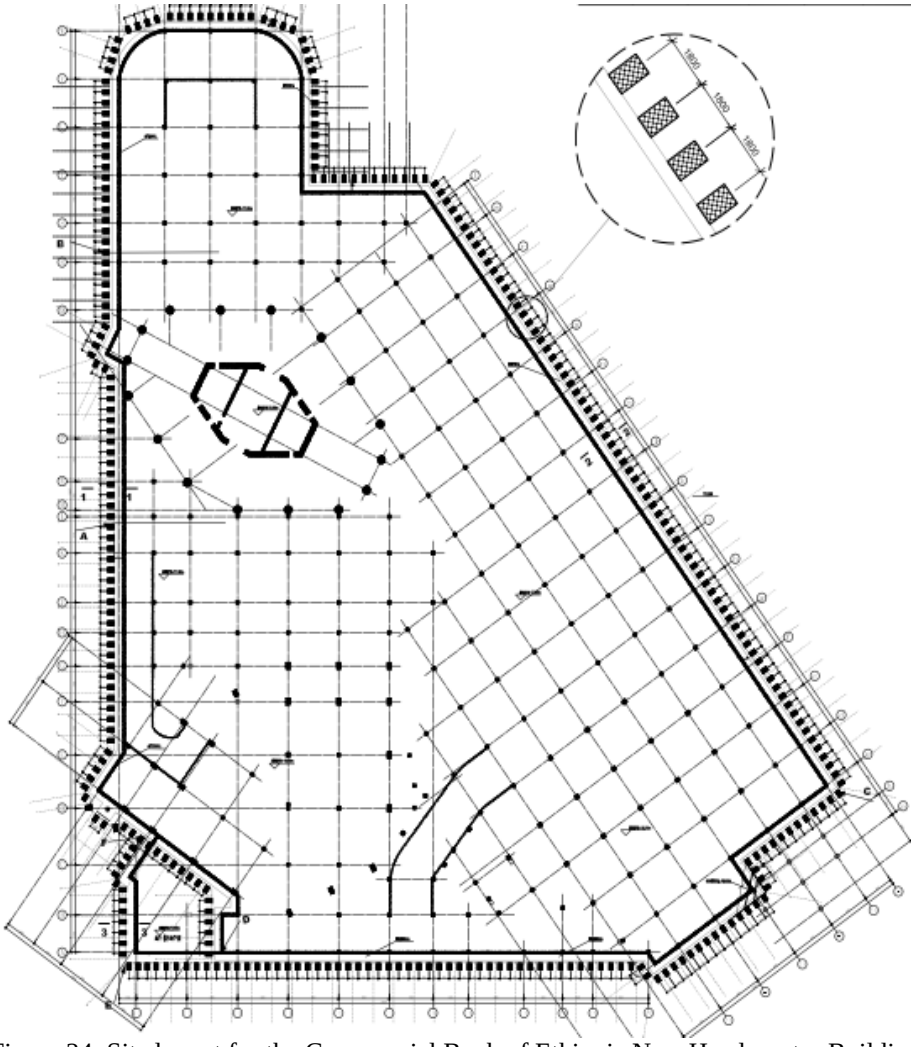

Figure 24: Site layout for the Commercial Bank of Ethiopia New Headquarter Building

V. CONCLUSION

The finite element programs Plaxis 2D and 3D were used in the modelling. Two different constitutive models in plaxis i.e. Hardening soil model and the Hardening soil model with small strain, were used to simulate the secant pile wall and soil behavior. The following conclusions have been drawn from the analysis:

The effect of stage excavation. The analysis for stage excavation showed that the deformations increased as the excavation depth increased. This was due to an increase in the magnitude of the unbalanced forces as a result of the increase in depth of excavation, thus increasing stresses and deformations.

A 3D model presents more realistic results than the 2D model. The 3D effects are not captured in a 2D model, which assumes plain strain conditions. Thus, excavation geometry and the loading condition can only be fully modelled using Plaxis 3D analysis.

REFERENCES

[1]. Atalay, A. (2016). Unpublished Seismic Investigation report for the CBE, new building site.
[2]. Bauduin, C., De Vos, M. & Frank, R. (2003). ULS and SLS de-sign of embedded walls according to Eurocode 7. Proc.XIII ECSMGE, Prague (Czech Republic), Vol. 2, 41- 46.
[3]. Brinkgreve, R.B.J., Swolfs, W.M., Engine, E. (2011). PlaxisUser˝s manual, PlaxisBv, the Netherlands
[4]. Clough, G.W., O˝Rourke, T.D. (1990). Construction Induced movement of in situ walls.Proc. Design And performance of earth retaining structure, ASCE special conference, Ithaca, New York, pp.439-470.
[5]. Emuriat, J.E. (2017). Parametric Study on Analysis and Design of Permanently Anchored Secant Pile Wall for Earthquake Loading. IJCER, SSN (e): 2250 – 3005 || Volume, 07 || Issue, 05|| May – 2017 ||.
[6]. Institution of Civil Engineers (ICE), 2007.Specification for pilling and Embedded Retaining Walls. Thomas Telford Ltd, second edition, 264p.
[7]. Moormann, C. (2004). Analysis of wall and ground movement due to deep excavation in soft Soils Based on a new worldwide data base. Soils and Foundations, voil.44, No.1, 87.
[8]. Perk, R.B. (1969). Deep excavation and tunneling in soft ground. In: proceeding of the 7th International conference on soil mechanics and Foundation engineering, Mexico City, State-of-The-Art Volume, pp225-290.

[9]. Schweiger, H.F. (2002). Results from numerical benchmark exercise in geotechnics. Proc. 5th European Conf. Numerical Methods in Geotechnical Engineering (P. Mestat, ed.), Presses Ponts Et chaussees, Paris, 305-314.
[10]. Schweiger, H.F. (2005). Application of FEM to ULS design (Eurocodes) in surface and near surface Geotechnical structures. Proc. 11th Int. Conference of IACMAG, Turin, Italy, Bologna: Patron Editore. 419-430.
[11]. Simpson, B. (2000). Partial factors: where to apply them? Proc. Int. Workshop on Limit State Design In Geotechnical Engineering, Melbourne, 145-154.
[12]. Spring (2011). Plaxis Bulletin/www.plaxis.nl
[13]. Suroor, Hadi. (2007). Performance Evaluation of Instrumented LNG Retention Dikes on Louisiana Soft clays. 7th International Symposium on Field Measurements in Geomechanics, Boston, USA.
[14]. Wood, D., Muir. (1990). Soil behavior and critical state soil mechanics. Cambridge University press. ISBN0-521-3249-4.